Effects of infrared radiation on the mechanical properties of an epoxy-amine adhesive using a Central Composite Design method

Sébastien Genty [a,b], Philippe Tingaut [b], Claire Tendero [a], Maëlenn Aufray [a,*]

[a] CIRIMAT, Université de Toulouse, CNRS, INPT, UPS, 4 Allée Émile Monso, BP44362, 31030, Toulouse Cedex 4, France
[b] SOCOMORE, ZI Du Prat, 56037, Vannes Cedex, France

ARTICLE INFO

Keywords:
Epoxy adhesive
Infrared curing
Central composite design
Three-point bending test
Tensile strength
Flexural strength

ABSTRACT

Recently, the aerospace industry has been facing many challenges, including an increase in the production rates to meet the market needs. In the context of adhesives and liquid shim applications, this means the possibility of on-demand curing. In other words, adhesives must cure slowly at room temperature and this process must be accelerated at any time to allow for the fastest polymerization possible. However, while on-demand curing is possible in several ways (ultraviolet radiation, induction, or microwave), the route chosen in this study is infrared (IR) radiation. This is because this method allows curing at low temperatures (i.e., around 50°C) and is universal, hence requiring no modification in the adhesive formulation.

Given that the acceleration of polymerization using thermal (temperature) and nonthermal (radiation–matter interaction) effects has been demonstrated in another study, it is now important to study the properties of such an adhesive after curing under IR radiation.

In this study, we measured the following properties: adherence on aluminum 2024-T3 via three-point bending, tensile strength and modulus, and flexural strength and modulus. We also studied the parameters of the IR lamp, including the lamp-adhesive distance and the rate and temperature of polymerization. For this purpose, a composite design of experiments was used, which generally has two main advantages: screening and response surface methodology. On the one hand, screening allows determining the factors, among those selected, that have a significant influence on the studied responses. At the same time, it allows determining the interactions (synergistic effects) between the influencing parameters. On the other hand, response surface methodology allows quantifying the influence of the parameters and determining the optimal ones.

1. Introduction

Polyepoxide adhesives are widely used in the aerospace industry for structural bonding and liquid shim applications [1]. However, currently, these two-component materials cure at room temperature and in a rather slow fashion (i.e., 5–10 h of curing time for an application time of less than 1 h). Therefore, to reduce the curing time of these adhesives without modifying their application time, it is necessary to consider on-demand curing methods, called COD [2]. In recent years, much attention has been paid to the new and so-called unconventional polymerization methods. Many of these methods are based either on heat transfer, such as induction polymerization [3–5] and microwave [6–10], or on reaction activation by electromagnetic radiation, such as ultraviolet radiation [11–13].

In this work, we chose infrared (IR) radiation as our preferred on-demand curing method because it eliminates the need for adding chemical compounds to the adhesive formulation, making this method versatile (i.e., applicable to products already on the market). The other advantage of IR radiation resides in the low inertia [14] (i.e., rapid temperature variation) and low energy consumption required to produce IR radiation [15]. In addition, IR radiation is effective in direct contact with adhesives and in areas where the adhesive is not directly exposed to the light source (shadow zone). Hence, depending on the needs and constraints, several IR sources whose line of sight is perpendicular to the surface of the adhesive can be used: a far-IR source (400–10 cm^{-1}), which heats the adhesive on the surface; a mid-IR source (4000–400 cm^{-1}), which heats the adhesive at the core; and a near-IR source (12,500–4000 cm^{-1}), which penetrates the adhesive until reaching the substrate and causes more homogeneous heating.

In a previous study [16], the kinetics of an epoxy-amine mixture

* Corresponding author.
E-mail address: maelenn.aufray@ensiacet.fr (M. Aufray).

https://doi.org/10.1016/j.ijadhadh.2021.102990

under IR radiation have been studied. IR polymerization has been shown to produce different curing kinetics from those observed with a simple increase in temperature. This additional IR effect was termed the nonthermal effect. Furthermore, after it has been demonstrated that the activation energy of the epoxide-amine reaction decreases under IR radiation, the most probable hypothesis suggested was that the epoxide functions to absorb IR radiation, causing local agitation at the reactive group, followed by an increase in reactivity without a "macroscopic" increase in temperature.

In this study, we focus on the mechanical properties (adherence, tensile and flexural strength at break, and tensile and flexural modulus) of a polyepoxy adhesive cured under IR radiation. The aim of the experiments is to identify which parameters influence the mechanical properties and to optimize these parameters to enhance the adhesive itself and its cohesive properties.

2. Experimental

2.1. Model adhesive

The polymer matrix that we used was a stoichiometric mixture between an epoxy prepolymer and an aliphatic amine hardener. The epoxy prepolymer (n 0.03) was a bisphenol A diglycidyl ether (DGEBA, epoxy equivalent weight 171–175 g·eq^{-1}; D.E.R.™ 332 from Dow Chemicals), and the hardener was triethylenetetramine (TETA, amine hydrogen equivalent weight 24 g·eq^{-1}; D.E.H.™ 24 from Dow Chemicals). The two chemical structures of these molecules used to form the model adhesive are shown in Fig. 1.

The model adhesive used in this study was a stoichiometric mixture of DGEBA with 13.9 parts per hundred grams of resin (*phr*) of TETA. Given these proportions, the infinite onset glass transition temperature measured using differential scanning calorimetry (i.e., at a conversion degree of 1.0) was 138°C.

2.2. Infrared curing

Fast curing was performed using an IR lamp supplied by Sunaero (Lyon, France). This method is already used industrially, in aeronautics, to accelerate the polymerization of sealants or for composite repairs [17]. This lamp was initially supplied to increase the kinetics of polymerization only via radiation energy transfer. It consists of a transportable control panel and an IR lamp emitter. The lamp is fixed on a tripod so that the line of sight of the IR radiation is perpendicular to the surface of the adhesive, and the distance between the lamp and the adhesive is adjustable. The induced temperatures, heat-up ramps, and heat times are set up in the control panel so that the emitted flux is automatically regulated by the temperature measurement of the cured sample with a K-type thermocouple. As previously outlined [16], IR emittance is mainly within the medium range (i.e., 400–4000 cm^{-1}), and the radiative flux is provided in Appendix B.

Under the usual conditions of use, the IR lamp is placed at approximately 20 cm from the adhesive to be cured and the temperature is increased at a rate of 5.5°C·min^{-1} until the adhesive reaches a temperature plateau of 50°C. Notably, the emitted flux in this mode has been previously measured and presented [16], and this way of curing is called IR-Φ_{Auto}.

For sample preparation and the measurement of the adhesive properties, the operating conditions are provided in the corresponding sections.

2.3. Mechanical characterization

All three mechanical tests described below were performed using a mechanical testing machine (Instron 3369, Élancourt, France) equipped with a 500 N sensor with a sensitivity of 0.5% for the measured values.

2.3.1. Three-point bending test

A three-point bending test was performed according to the ISO 14679:1997 [18–20] standard. This test helps determine the ability of a material to adhere to a substrate. It involves bending a rectangular polymer block (25 mm in length and 5 mm in width) bonded to the surface of a substrate (40 mm in length and 10 mm in width). For this study, although the thickness of the substrate is not specified by the standard, it was chosen as 1 mm of aluminum alloy 2024-T3. Then, the three-point bending specimens are tested at room temperature at a speed of 0.5 ± 0.001 mm min^{-1}.

It should be noted, however, that to measure the adhesion of a model adhesive under an IR lamp, the preparation setting differs slightly from that indicated by the standard. Indeed, different curing process types (oven or IR radiation) can lead to different conversion rates and, therefore, different adhesive modulus values. As shown in Fig. 2, the load at break (F_{Max}) depends not only on the adherence (W_{Adh}) itself, but also on the stiffness of the substrates ($W_{Substrate}$). Thus, measuring the adherence value by studying F_{Max} is only possible if the stiffness of the substrate and that of the rectangular block remain the same from one experiment to the other.

Therefore, it is important to ensure that the rectangular block is cured under the same conditions across all tests to obtain an identical conversion rate. Hence, a new preparation setting for the three-point bending specimen has been proposed. In this method, on a degreased, deoxidized, sol-gel-coated aluminum alloy [22], the model adhesive is applied at a thickness of 0.3 mm using spacers on both sides of the substrate. The sample is then placed immediately under an IR lamp to initiate the curing process. Once polymerization has been realized, three-point bending rectangular blocks are manufactured in accordance with ISO 14679:1997 [18–20] and cured in an oven. Fig. 3 shows the method chosen for preparing the adherence samples after curing under IR radiation.

It is worth noting that after curing in the oven, the adhesives and rectangular blocks are not completely cured, since the T_g value of the

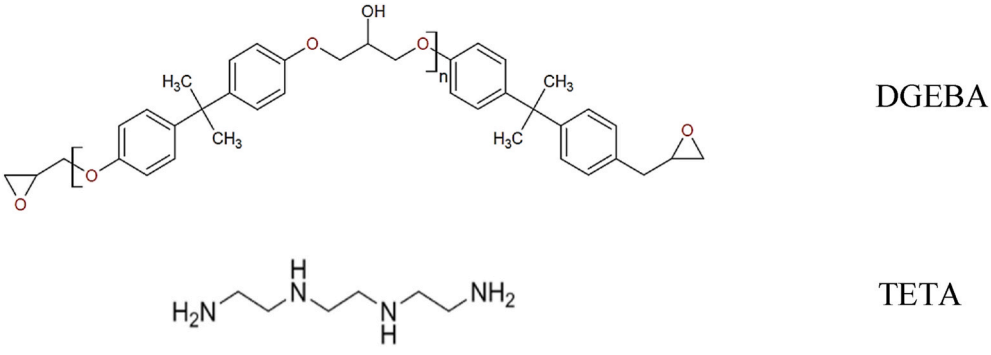

Fig. 1. Chemical structures of the DGEBA and TETA molecules.

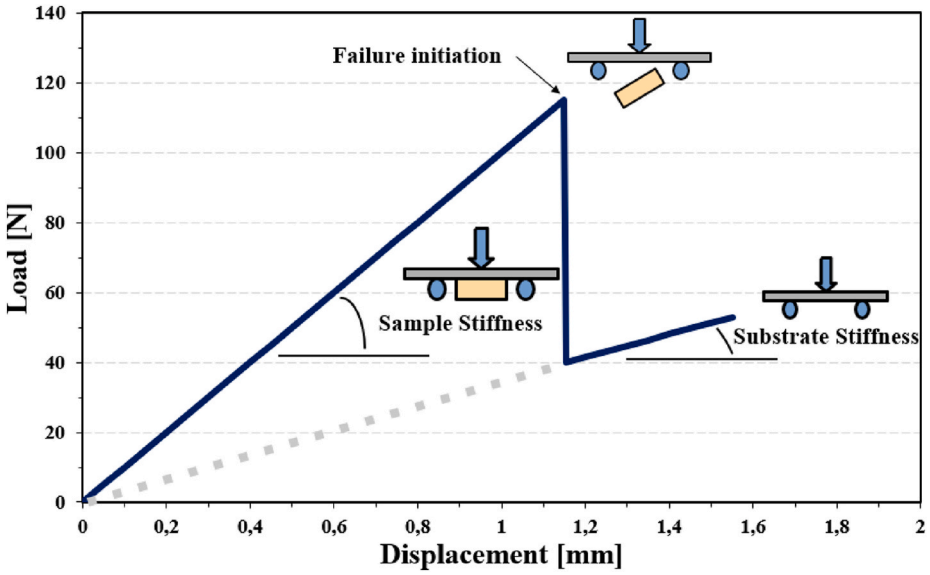

Fig. 2. Illustration of the load–displacement curve for a three-point bending adherence test, highlighting the stiffness of the sample and substrate according to [21].

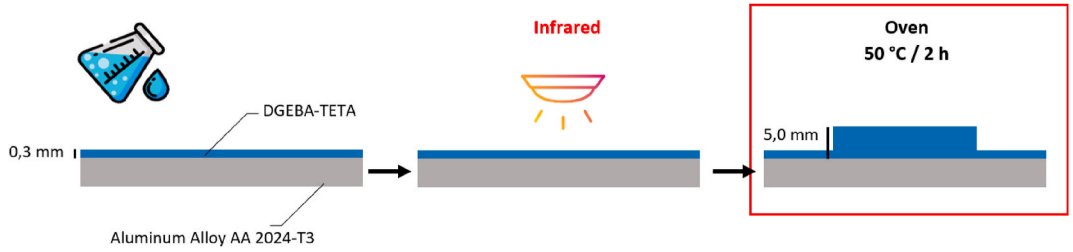

Fig. 3. Method used for preparing three-point bending samples.

model adhesive cured under IR radiation is 85°C while it is $T_{g\infty}$ 138°C when fully cured. Generally speaking, the aim in this study is to assess the influence of the curing parameters on the final mechanical properties, regardless of the degree of curing. Therefore, since the stiffness of the rectangular block always remains the same, using a constant temperature in each trial allows the results to be reproducible.

2.3.2. *Tensile strength and modulus*

Dumbbell-type specimens were molded by pouring epoxy-amine monomers into a silicon mold and then placed directly under an IR lamp, according to the various parameters considered in this study. To control the IR emission, a thermocouple was placed at the end of the sample, in an area that would not interfere with the mechanical test.

The test was performed in accordance with ISO 37:2017 at a speed of 0.5 ± 0.001 mm min^{-1}. Fig. 4 shows the dimensions of the manufactured samples.

Data on the tensile strength and elastic modulus were collected from these tests. Both the tensile strength (σ_r, in MPa) and the elastic modulus (E, in MPa) were determined according to Equation (1) and Equation (2), respectively:

$$\sigma_r \quad \frac{F_r}{l \times e} \qquad \text{Equation 1}$$

$$E \quad \frac{\Delta F}{l \times e \times \Delta\varepsilon} \qquad \text{Equation 2}$$

where F_r is the load at break (N), l and e are, respectively, the initial width and thickness of the specimen (both in mm), and ΔF (N) is the difference in the force applied in each deformation range $\Delta\varepsilon$ (between 0.25% and 0.5%, as proposed in NF ISO 527–2).

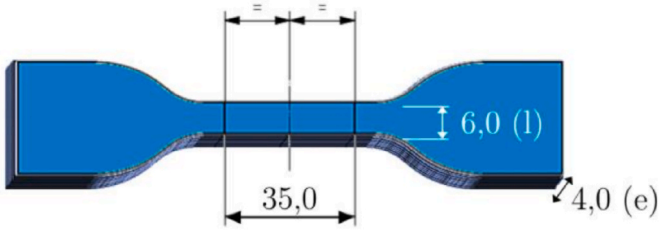

Fig. 4. Dumbbell samples used to determine the tensile strength and modulus (dimensions in mm).

2.3.3. *Flexural strength and modulus*

Beam-type specimens were molded by pouring epoxy-amine monomers into a silicon mold and then placed directly under an IR lamp, according to the various parameters considered in this study. To control the IR emission, a thermocouple was placed at the end of the sample, in an area that would not interfere with the mechanical test.

Both the load at break and flexural modulus values were determined using a three-point bending test on beam specimens, as outlined by ISO 178:2010. According to this standard, the beam dimensions for samples of thermosetting materials are a cross section of 3.2 mm by 12.7 mm and a length of 127 mm.

Both the tensile strength (σ_f, in MPa) and the elastic modulus (E_f, in MPa) were determined according to Equation (3) and Equation (4), respectively:

$$\sigma_f \quad \frac{3.F_f.L}{2.b.d^2} \qquad \text{Equation 3}$$

$$E_f \quad \frac{L^3.m}{4.b.d^3} \qquad \text{Equation 4}$$

where F_f is the load at break (N), L is the distance between supports (mm), b and d are, respectively, the width and thickness of the beam-type specimen (mm), and m is the slope of the deformation–load curve (i.e., $m \quad \frac{|\Delta F|}{|\Delta f|}$, with f for deformation in mm). Thus, the values of σ_f and E_f can be calculated from the breaking force F_f, obtained graphically on the bending curves. It is important to note that for this test, the deflection (and, consequently, the flexural modulus) is determined by the displacement of the crossbeam.

2.4. Design of experiments

By varying all the parameters for each experiment and conducting a statistical study, the design of experiments (DoE) allows many factors to be studied and correlated with a minimum number of tests. It also allows modeling the studied responses and suggesting an optimization for the experimental parameters from the established models [23]. A composite DoE was selected as it allows a second-order polynomial equation to model the effects of various factors. Besides, among all the designs that allow second-order polynomials, this design is the one with the least variance and no covariance. In other words, this design allows properly calculating the effect of each factor, even if the constant a0 is not perfectly calculated. All DoE data were processed using Design-Expert® software version 10, and all the influential factors were also directly determined on it. To determine the influence of IR polymerization parameters, the effects of three factors were studied: the distance between the IR emitter and the sample in centimeters (A), the induced temperature of the adhesive in °C (B), and the heating rate to reach the correct temperature in °C/min (C). All the factors and associated levels are presented in Table 1. For axial points, α levels are used, which in this DoE are set at ±1.32.

It should be noted that these three factors have been chosen for two specific reasons. First, these are the three parameters that the lamp user can control. Thus, from an industrial standpoint, it is possible to suggest an optimized lamp configuration to obtain the desired mechanical properties. However, above all, these parameters allow the effects of temperature and radiative flux to be uncorrelated; in other words, both the thermal and nonthermal effects should be investigated separately. Indeed, the heating rate and distance factor have an impact on the radiative flux emitted, initially during the first minutes (i.e., the low conversion rates) and then for the entire duration of the test. Finally, the temperature factor has an impact on both the thermal and nonthermal effects at the same time. Therefore, studying significant factors can help determine the role of thermal and nonthermal effects in the evolution of mechanical properties.

Thus, the thermal effect of IR radiation (only the increase in temperature) is explained with temperature (factor B) as a unique influential parameter. If the temperature factor is significant with AC, AB, or BC interactions, then the thermal and nonthermal (coupled) effects will be at the origin of the response variations. However, if the influencing factors are parameters A and C or their quadratic effects or respective interactions, then only the nonthermal effect will cause variations in the mechanical properties.

Table 2 provides the number of tests performed according to the DoE. For each experiment, four specimens were prepared simultaneously under the same conditions. This allowed obtaining an average value for the four samples. The DoE-01 to DoE-06 series correspond to different tests with the same factor values. This allows determining whether the answers studied yield reproducible results and are adapted to the chosen DoE methodology. In other words, it allows testing the reliability of the system. Thus, these six trials allow determining the level of uncertainty. However, it is important to note that all six of these points were not considered for the resolution of the DoE, with the exception of the first experiment, DoE-01. In addition, other series were performed several times at different dates to check the level of reproducibility. The results showed that the DoE-11 and DoE-12 series correspond to the same parameters, as well as the DoE-17 and DoE-18 series.

For each series of tests, five answers were studied: adherence (three-point bending), tensile properties (tensile strength and modulus), and flexural properties (flexural strength and modulus), and for each answer, four samples were evaluated. For each result, an analysis of variance (ANOVA) was performed.

For this purpose, in the Design-Expert® software, the Fisher factor (F) is provided for each response analysis. This factor corresponds to the ratio between the sum of the squares of the model and the sum of the squares of the residues. Then, the p-value is defined by the probability of observing F if the null hypothesis H_0 is verified, and it was set at 5% (p-value less than 0.05).

ANOVA was performed in two rounds with the Design-Expert® software. First, it was performed in a raw form with the available data. Thus, a p-value was calculated for each of the parameters. A p-value less than 0.05 (i.e., a confidence level of more than 95%) was considered to confirm the significance of factors. Thus, a new ANOVA (Round 2) was performed with only those parameters whose p-value was less than 5%. Table 3 shows the ANOVA (both Round 1 and Round 2) results for the three-point bending adherence tests as an example.

In this example, the resolution of the DoE in the Design-Expert® software shows that the significant terms are the C parameters (heating rate for a p-value less than 0.0001). Both of the A^2 parameter (the

Table 1
Factors and levels chosen for the DoE.

Factors	Levels				
	−α	−1	0	+1	+α
(A) Distance [cm]	16.8	20.0	30.0	40.0	43.1
(B) Temperature [°C]	45.2	50.0	65.0	80.0	84.7
(C) Heating rate [°C/min]	2.2	3	5.5	8	8.8

Table 2
List of tests of the DoE. The first row (colored in red and underlined) is the reference point that is outside the DoE, whereas the labels written in italics are iterations.

Number	A	B	C	(A) Distance [cm]	(B) Temperature [°C]	(C) Heating rate [°C/min]
IR-Φ_{Auto}	N/A	N/A	N/A	25	50	5.5
DoE-01	0	0	0	30	65	5.5
DoE-02	*0*	*0*	*0*	*30*	*65*	*5.5*
DoE-03	*0*	*0*	*0*	*30*	*65*	*5.5*
DoE-04	*0*	*0*	*0*	*30*	*65*	*5.5*
DoE-05	*0*	*0*	*0*	*30*	*65*	*5.5*
DoE-06	*0*	*0*	*0*	*30*	*65*	*5.5*
DoE-07	+1	−1	+1	40	50	8
DoE-08	−1	−1	+1	20	50	8
DoE-09	−1	−1	−1	20	50	3
DoE-10	+1	−1	−1	40	50	3
DoE-11	0	−α	0	30	45.2	5.5
DoE-12	*0*	*−α*	*0*	*30*	*45.2*	*5.5*
DoE-13	+α	0	0	43.1	65	5.5
DoE-14	−α	0	0	16.8	65	5.5
DoE-15	0	0	−α	30	65	2.2
DoE-16	0	0	+α	30	65	8.8
DoE-17	0	+α	0	30	84.7	5.5
DoE-18	*0*	*+α*	*0*	*30*	*84.7*	*5.5*
DoE-19	−1	+1	−1	20	80	3
DoE-20	−1	+1	+1	20	80	8
DoE-21	+1	+1	+1	40	80	8
DoE-22	+1	+1	−1	40	80	3

Table 3
ANOVA results for the three-point bending adherence tests.

Factors/ interactions	F (Round 1)	*p*-value (Round 1)	F (Round 2)	*p*-value (Round 2)
A	2.52	0.1466	2.83	0.1203
B	1.25	0.3418		
C	**31.87**	**0.0003**	**35.68**	**<0.0001**
AB	0.83	0.3872		
BC	0.11	0.7520		
AC	**9.63**	**0.0127**	**10.78**	**0.0071**
A^2	**2.63**	**0.1789**	**11.64**	**0.0041**
B^2	0.27	0.6356		
C^2	1.29	0.3183		
***R* squared**			**83%**	
Adj. *R* squared			**77%**	

quadratic effect of the distance for a *p*-value of 0.0041) and the A and C parameters are correlated and significant (a *p*-value of 0.0071 for the distance/ramp correlation). Factor A (the distance for a *p*-value of 0.1203) should be included in the analysis because of the requirement of the model hierarchy as it has an interaction effect. Fig. 5 represents the normal probability of studentized residuals for adherence. Each point corresponds to a test conducted experimentally, and the real value of each point can be identified by its color (from blue to red for values between 106 and 327 N, respectively), the line representing the model. As can be seen, the points are close to the normal line, which means that the errors are distributed normally, and the model is appropriate.

This means that using a model allows predicting the results for any parameter values contained in the test design. Thus, an optimization for the process parameters is suggested.

3. Results and discussion

3.1. Thermal versus infrared curing

In the first step, before the DoE was performed, IR polymerization (IR-Φ_{Auto}) was compared to pure thermal curing (50°C). IR curing was achieved at a distance of 20 cm with an increase in temperature at a rate of 5.5°C·min^{-1} and a maximum temperature of 50 °C in the stationary mode. This first step was performed to highlight the effects of IR radiation, regardless of the parameters modified in the later part of the article.

For these two methods of curing, four samples were manufactured for each of the mechanical properties tested: three-point bending adherence and flexural and tensile stress/strain properties. All the results are presented in Fig. 6.

Starting with the analysis of the adherence results (first series of columns), all samples tested up to rupture were found to exhibit an interfacial fracture (i.e., the fracture looked adhesive to the naked eye). The loads at break were, therefore, representative of the adherence (adhesive initiation of fracture) for both curing pathways. Apart from uncertainty, the load required for the initiation of rupture was the same for both polymerization pathways. In other words, the level of adherence following IR curing was the same as that following thermal curing. Therefore, from these first tests, it seems that IR radiation does not significantly modify the polymer–metal interaction. For the purpose of comparison, in the literature, microwave polymerization (which is also characterized by a nonthermal effect) was found to result in an increase in the adherence measured by a single lap joint test [9]. This non difference in adherence after IR curing was unexpected, as it has previously been observed that the interphase formation (i.e., the reaction between an amine and an aluminum surface) decreases the adherence [20]. Indeed, when an epoxy-amine mixture is cured on an aluminum alloy surface, a competition arises between polymerization and the reaction between the amine and the metal [24], and an interphase is created [20,24,25]. Hence, it is reasonable to believe that a modification of the kinetics, and therefore of the vitrification, leads to a modification of this interphase, as well as of the internal stresses and consequently the adherence.

Now, the flexural strength at break (second series of columns) was found to increase by more than 20% with IR curing (146 ± 15 MPa compared to 120 ± 13 MPa). This phenomenon has already been observed in the case of microwave polymerization of Carbon Fiber Reinforced Polymer (CFRP) [26]. In the case of the composite studied, the flexural strength at break was found to evolve from 1552 ± 44 MPa under microwave to 1326 ± 29 MPa under pure thermal conditions. In that study, Xu showed that the increase observed in the strength at break is explained by the decrease in the quantity of air present in the material (air bubbles). Thus, in an autoclave (under vacuum), the flexural strength at break was found to increase to 1651 ± 32 MPa. In our study, the presence of air bubbles and the internal constraints (both can be linked) are two serious avenues explaining the increase in the flexural strength at break of the DGEBA-TETA mixture. The flexural modulus (third series of columns) of the DGEBA-TETA mixture cured under IR radiation was found to be the same as that under thermal curing.

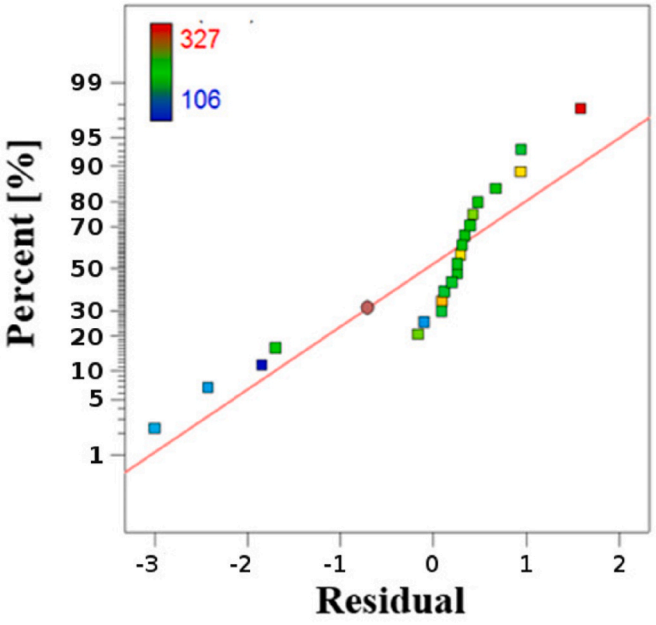

Fig. 5. "Studentized" residuals plot for adherence data measured in three-point bending.

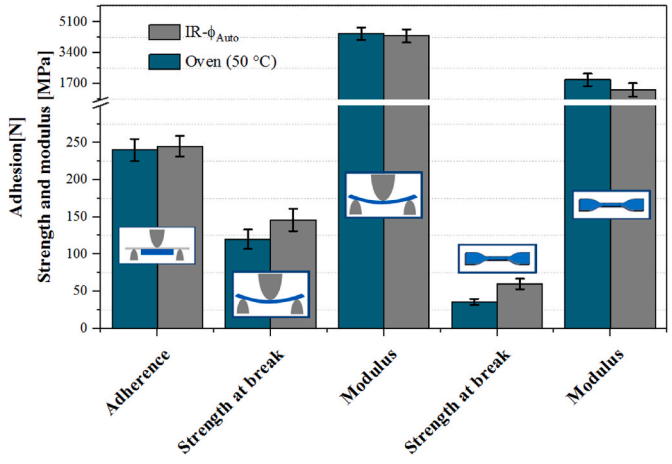

Fig. 6. Some mechanical characteristics of the DGEBA-TETA mixture according to both methods of curing (IR-Φ_{Auto} and thermal curing).

Generally, IR radiation allows obtaining a material with a higher tensile strength (+60%), in comparison to pure thermal cured adhesive. However, it also exhibits a module that is the same as thermal curing, apart from uncertainty. The increase observed in the mechanical tensile properties has already been observed in the case of IR curing [23]. The explanation provided in the case of this study, which seems compatible with the IR lamp polymerization performed in this work, consists of more homogeneous IR curing resulting in a reduction in the residual stresses in the material. It is also worth noting that some similarities have already been observed when microwave curing was considered. Thus, it can be concluded that microwave radiation leads to a modification of the mechanical properties of adhesives by releasing the internal stresses [27].

3.2. The role of infrared lamp parameters (DoE)

During IR curing, the changes that occur in the mechanical properties may be a combination of thermal and nonthermal effects. To study the effects of IR radiation more accurately, the effects of temperature (thermal effects) should be uncorrelated to those of radiative flux (nonthermal effects). However, since this is not experimentally feasible, using a DoE with a Central Composite Design (CCD) is proposed. This allows the investigation of influencing factors while considering quadratic effects in a minimum number of testing. The results of the experimental tests for adherence, tensile and flexural strength at break, and tensile and flexural modulus are available in Appendix A. Each line corresponds to an average of four samples with the same batch number (i.e., performed at the same time), and the errors for each of the properties are defined by the standard deviation of all the specimens from DoE-1 to DoE-6 (i.e., 24 (6 × 4) specimens).

3.2.1. Adherence

Given the adherence results obtained in three-point bending (last column of the table), the resolution of the DoE in the Design-Expert® software shows that the significant terms, which are the heating rate (parameter C for a p-value less than 0.0001), the square of the distance parameter (the quadratic effect of parameter A for a p-value of 0.0041), and the distance and heating rate (a p-value of 0.0071 for the distance–ramp correlation), are correlated and significant. Notably, the distance (parameter A for a p-value of 0.1203) should be included in the analysis because of the requirement of the model hierarchy as it has an interaction effect. The final equation with the coded factors for predicting the adherence of the DGEBA-TETA mixture after IR curing is provided in Equation (5), and the same equation with the real factors (in cm for the distance and °C/min for the heating rate) is provided in Equation (6):

$$Adh.[N] \quad 197.7 \quad 9.7A + 34.4C + 22.6AC + 37.7A^2 \qquad \text{Equation 5}$$

$$Adh.[N] \quad 484 \quad 18.4 \times Distance \quad 13.4 \times Heatingrate + 0.9 \times Distance \times Heatingrate + 0.2 \times Distance^2 \qquad \text{Equation 6}$$

It is worth noting that the distribution of studentized residuals is in line with the theoretical values from Equation (5) and Equation (6). Therefore, within the limits of the parameters used for the DoE, these equations can be used to predict the adherence of the DGEBA-TETA mixture on AA 2024-T3 after IR curing.

Fig. 7 shows adherence as a function of the AC parameters for a temperature value set at 65 °C.

Indeed, the dependence of the adherence on the heating rate (C) and the combined effect of the heating rate and distance (parameter AC) are easily observable. The value of adherence increases to 275 N for the maximum heating rate and distance to just over 150 N for the minimum heating rate and maximum distance. It is worth noting that both the distance and heating rate have a significant influence on the energy received by the adhesive. Moreover, at a constant heating rate, the adherence values change a little as a function of the distance parameter alone (parameter A not significant).

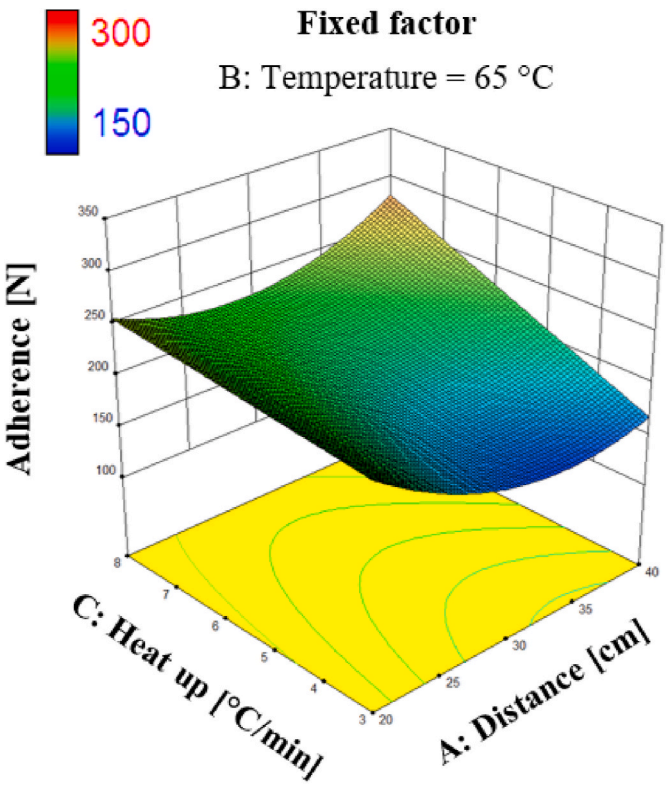

Fig. 7. Influence of the parameters on the measurement of the three-point bending according to parameter AC.

The DoE shows that IR curing leads to a change in adherence (from 150 to 300 N, depending on the parameters used). This first response from the DoE, however, does not confirm the observations made in the simple comparison between thermal and IR curing (cf. Fig. 6). Recall that IR curing did not change the adherence level of the DGEBA-TETA mixture on AA 2024-T3 (240 and 255 N, respectively). Therefore, the resolution of the DoE allows determining whether IR radiation (i.e., nonthermal effect) modifies the level of adherence and, hence, the substrate–adhesive interaction. In addition, by further studying the significant factors, it was found that it is the nonthermal effect that causes a change in adherence with the heating rate (parameter C), distance (parameter A), and their interaction (parameter AC) as significant factors. Thus, high radiative flux at the beginning of curing (i.e., a high heating rate) leads to a significant increase in adherence.

3.2.2. Tensile strength

The tests performed according to the DoE show that parameters A and C are significant (distance and ramp for p-values of 0.0002 and 0.0482, respectively) and that the correlation of distance (parameter A) and temperature (parameter B) is also significant (with a p-value of 0.0013). The final equation with the coded factors for the prediction of

the tensile strength of the DGEBA-TETA mixture after IR polymerization is provided in Equation (7), and the same equation with the real factors (in cm for the distance, °C/min for the heating rate, and °C for the temperature) is provided in Equation (8):

$$\sigma_r[MPa] \quad 44.45 + 8.09A \quad 5.63B + 2.00C + 8.56AB \qquad \text{Equation 7}$$

$$\sigma_r[MPa] \quad 8.54 \quad 0.18 \times Distance \quad 0.81 \times Temperature + 0.799 \times Heatingrate + 7.19.10^{\ 3} \times Distance \times Temperature \qquad \text{Equation 8}$$

According to parameters A, B, C, and AB of Equation (7) and Equation (8), the tensile strength values are well in line with the tensile strength measured in the DoE tests. This means that the determined model is reliable for predicting the tensile strength according to the distance, heating rate, and temperature parameters contained in the terminals as used in the DoE.

Besides, the tensile strength at break is expressed as a function of distance (parameter A) and temperature (parameter B) in Fig. 8, whose heating rate (parameter C) is set at 5.5°C/min.

The correlation between the distance (parameter A) and temperature (parameter B) can be observed on this graph with a significant increase in the fracture strength when the temperature decreases at a short distance as well as a slight decrease in strength when the temperature decreases at a larger distance. Although parameter AB is significant, the temperature (factor B) is not, whereas the distance (parameter A) and heating rate (parameter C) are. This clearly indicates that the variation in the tensile strength is governed by the nonthermal effect of IR radiation.

3.2.3. *Tensile modulus*

Among the parameters of the DoE, only the correlation of temperature (parameter B) and heating rate (parameter C), that is, parameter BC, is significant on the tensile modulus response (with a *p*-value of 0.0211). The final equation with the coded factors for the prediction of the modulus of the DGEBA-TETA mixture after IR polymerization is provided in Equation (9), and the same equation with the real factors (in °C/min for the heating rate and °C for the temperature) is provided in Equation (10):

$$E_r[GPa] \quad 1.74 + 3.1110^{\ 3}B + 0.06C \quad 0.093BC \quad 0.10B^2 \qquad \text{Equation 9}$$

$$E_r[GPa] \quad 1.02 + 0.067 \times Temperature + 0.186 \times Heatingrate \quad 2.4810^{\ 3} \times Temperature \times Heatingrate \qquad \text{Equation 10}$$

Although the BC factor is significant, the weight of this factor on the model is small. In other words, the influence of radiation (i.e., the nonthermal effect) on the flexural modulus is not evident, and if it exists, it is negligible and cannot be used to optimize the modulus values. Studying studentized residues revealed a very good match between the model and experimental data, proving that the suggested model is robust. Fig. 9 expresses the module in tension as a function of parameters B and C.

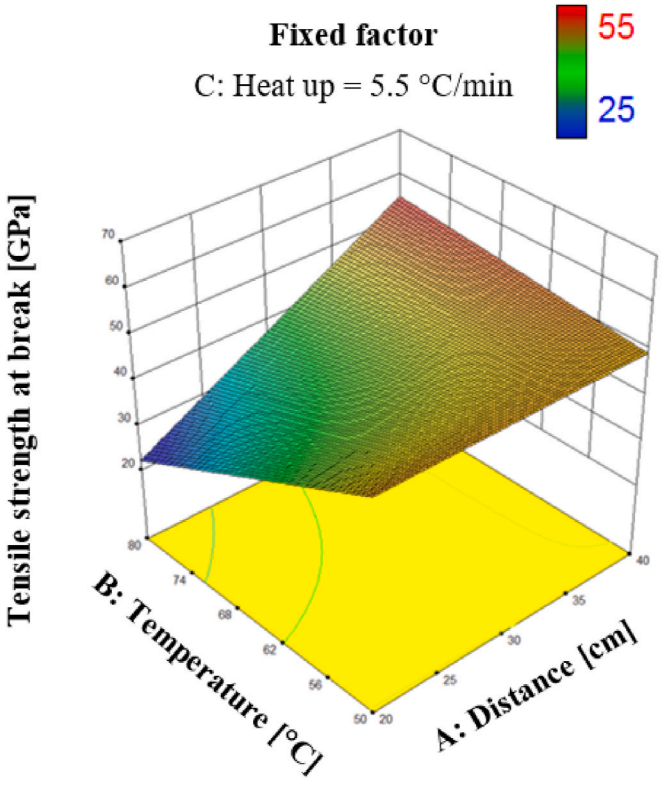

Fig. 8. Influence of the parameters on the measurement of the tensile strength at break according to parameter AB.

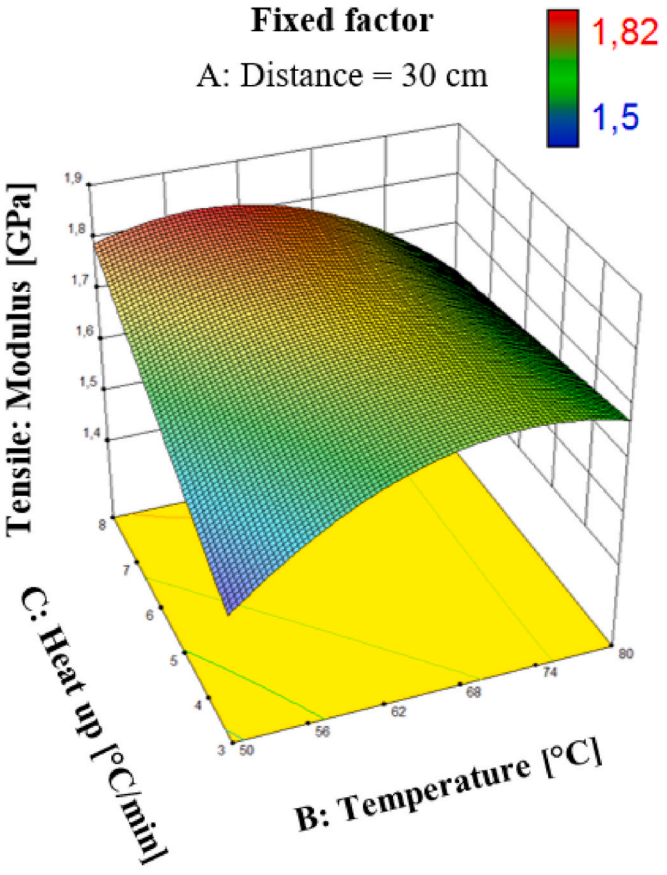

Fig. 9. Influence of the parameters on the measurement of the tensile modulus according to parameter BC.

It can be observed that parameters B and C separately are not significant and that it is their correlation that plays a role in the response studied.

3.2.4. Flexural strength

The resolution of the DoE shows that the significant factors for flexural failure strength are the temperature and distance. It also shows that the significant terms are the temperature (parameter B for a *p*-value of 0.0009), the quadratic effect of temperature (parameter B^2 for a *p*-value of 0.0009), and the quadratic effect of the heating rate (parameter C^2 for a *p*-value of 0.0263). However, parameters A and C alone are not significant, but parameter AB is to a lesser extent (a *p*-value of 0.0993). The final equation with the coded factors for predicting the flexural strength of the DGEBA-TETA mixture after IR curing is provided in Equation (11), and the same equation with the real factors is provided in Equation (12):

$$\sigma_y[MPa] \quad 148.83 + 0.21A \quad 19.92B \quad 0.43C + 12.79AB \quad 21.65B^2 \quad 14.76C^2$$

Equation 11

$$\sigma_y[MPa] \quad 76.26 \quad 5.52 \times Dis\tan ce + 8.62 \times Temperature + 25.79 \times Heatingrate + 0.08 \times Dis\tan ce \times Temperature \quad 0.096 \times Temperature^2 \quad 2.36 \times Heatingrate^2$$

Equation 12

It is worth noting that the flexural strength prediction model as a function of on-demand curing parameters using IR radiation is reliable. Indeed, the studentized residues are in accordance with the theoretical values of the model represented by the red line. In Fig. 10, the flexural strength is expressed as a function of distance (parameter A) and temperature (parameter B), with parameter A being significant and parameter AB not very significant, for a fixed heating rate of 5.5°C/min.

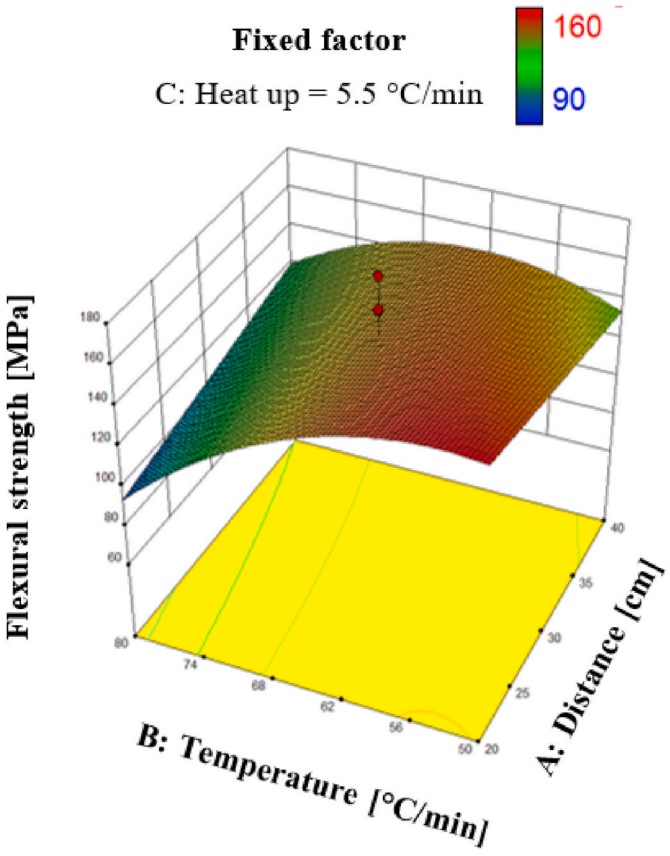

Fig. 10. Influence of the parameters on the three-point bending test according to parameter AC.

Thanks to the DoE and Design-Expert® software, it was demonstrated that none of the parameters of the DoE is significant for the results of the bending modulus. Here, the model is not realistic because the experimental dispersion is smaller than the uncertainty. Therefore, the lamp parameters do not allow, besides control, the induced temperature to optimize the value of the flexural modulus. In other words, the nonthermal effect does not lead to any change in the flexural modulus value.

3.3. Optimization of IR lamp parameters (DoE)

The objective here is to determine the experimental parameters of the IR lamp to optimize the properties of the adhesive cured by IR radiation. For this purpose, the equations that have previously been obtained are reused.

3.3.1. Verification of the previously established models

Before initiating the optimization tests, it is important to ensure that the results obtained under the conditions of the IR-Φ_{Auto} reference test are consistent with those predicted by the models in the DoE. This validation is particularly important since the conditions of the reference test (IR-Φ_{Auto}: 50°C with a distance of 25 cm and a heating rate of 5.5°C/min) are not part of the cube of the DoE. Table 4 outlines all of these results.

The results showed that the correlation between the properties predicted by the model and those measured in practice is very good for the flexural strength at break and adherence (less than 5% difference). Moreover, the predictions of the tensile strength at break and modulus were found to be acceptable (less than 10% deviation). Therefore, the predicted results are quite accurate as the error is below 10%, and hence the model can be considered as valid for further calculations and optimization.

From the model equations, it is possible to fix some input data and classify the desired responses according to their importance. Several scenarios have been developed, and some information is presented to analyze the optimization results. First, the optimal parameters are presented on diagrams with the minimum and maximum values of the DoE. It should be noted that all optimizations are included in the experimental domain (i.e., the presence of points outside the cube is not possible). Thus, the optimum value (—●— for factors and —●— for answers) is located on a diagram whose minimum value of the DoE is on the left and the maximum value is on the right. Studying the position of the responses in the experimental domain allows calculating the desirability, which corresponds to the average of the positions of each of the responses.

3.3.2. First optimization

The first optimization determines the lamp parameters to obtain an adhesive with the highest mechanical properties. For this purpose, the selected input data are a distance between 20 and 40 cm, a temperature between 40°C and 100°C, and a heating rate between 2°C/min and 10°C/min, all with no optimum required. Fig. 11 presents the optimal parameters and associated responses. Recall that desirability represents

Table 4
Results of the mechanical properties of the IR-cured adhesive (IR-ΦAuto) compared to the predictions provided by the model.

	σ_r [MPa]	E [GPa]	σ_f [MPa]	E_f [GPa]	F_{Max} [N]
Experimental data	60 ± 7	1.8 ± 0.4	146 ± 15	4.3 ± 0.5	255 ± 14
Predicted data (DoE)	55 ± 9	1.7 ± 0.1	153 ± 14	N/A	251
% Error	8.5	5.5	4.8	N/A	1.5

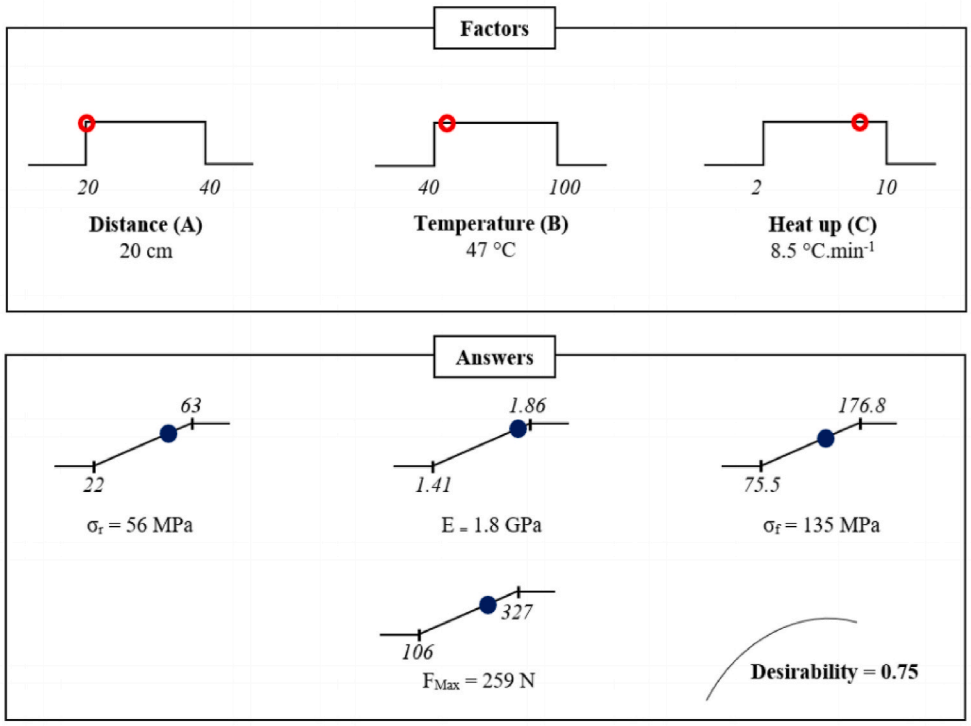

Fig. 11. IR lamp parameters calculated using models from the DoE.

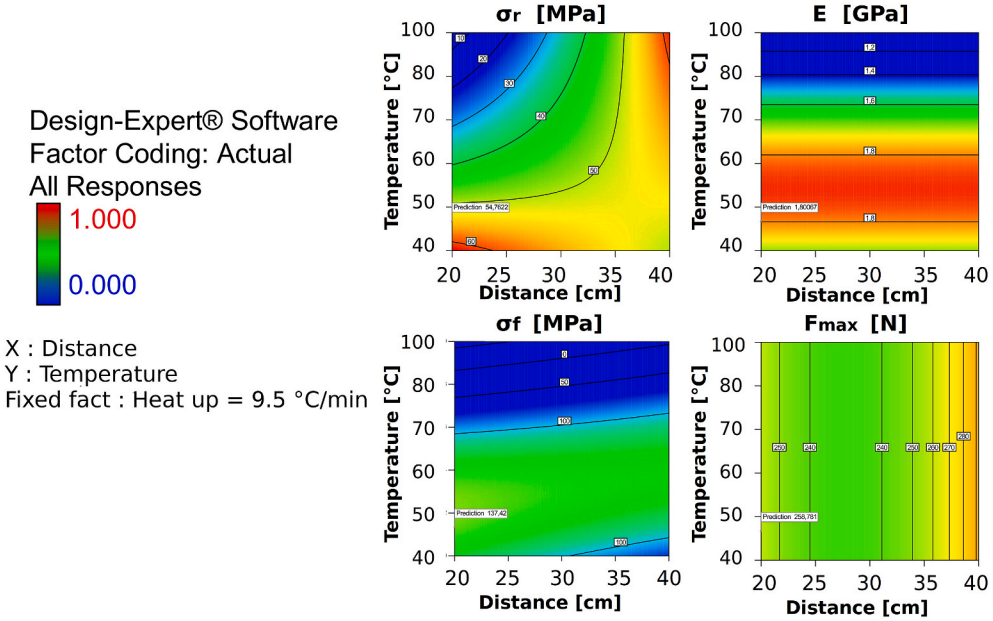

Fig. 12. Influence of temperature and distance on the results from the optimization.

the degree of satisfaction with the results of the model as a function of the maximum value that can be achieved (maximum value observed in the DoE). For this first optimization, the desirability is 75%, which means that, on average, the predicted mechanical properties are at 75% of their maximum value. Desirability represents the degree of satisfaction with the results of the model as a function of the maximum value that can be achieved. This index is equal to 0 if the value of the modeled response is outside the tolerance interval associated with it.

According to the models determined from the DoE data, the optimal lamp parameters are a distance between the sample and transmitter of 20 cm, a heating rate of 8.4°C/min, and an induced temperature of 47°C. Fig. 12 shows the influence of the temperature and distance parameter evolution on this optimization as a 2D plot.

In general, the most sensitive parameter in optimization is the temperature. Indeed, the results change a little if the distance is changed. In addition, temperature is regarded as a determining factor, and any small change in it leads to large variations in responses.

3.3.3. *Second optimization*

The purpose of this second optimization is to determine the optimal

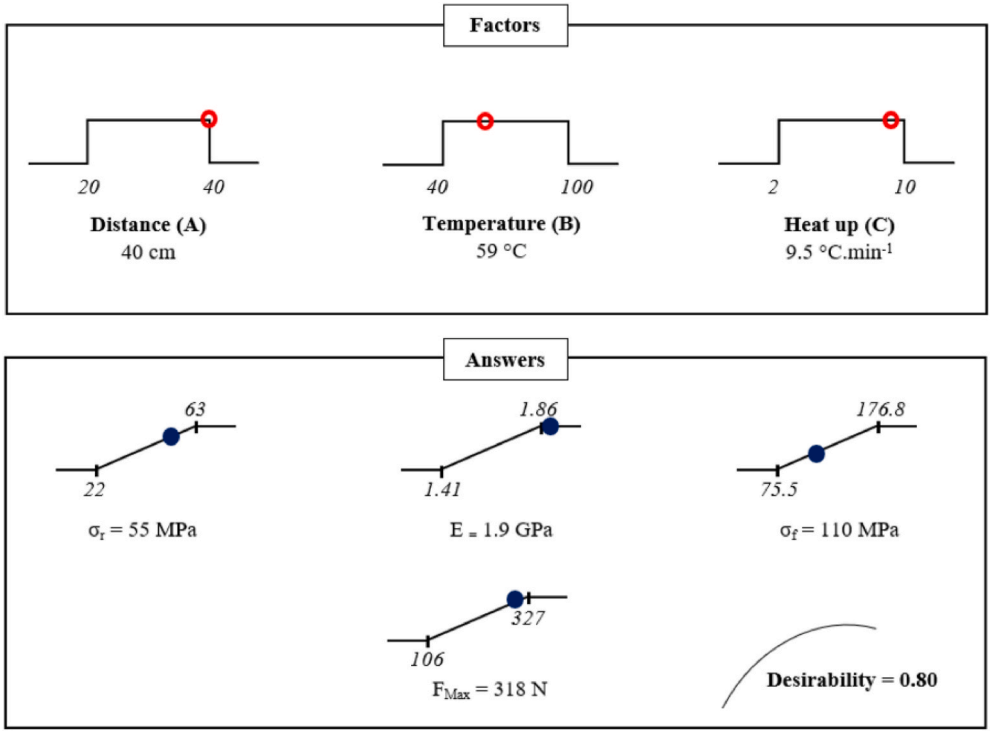

Fig. 13. IR lamp parameters calculated using the models from the DoE.

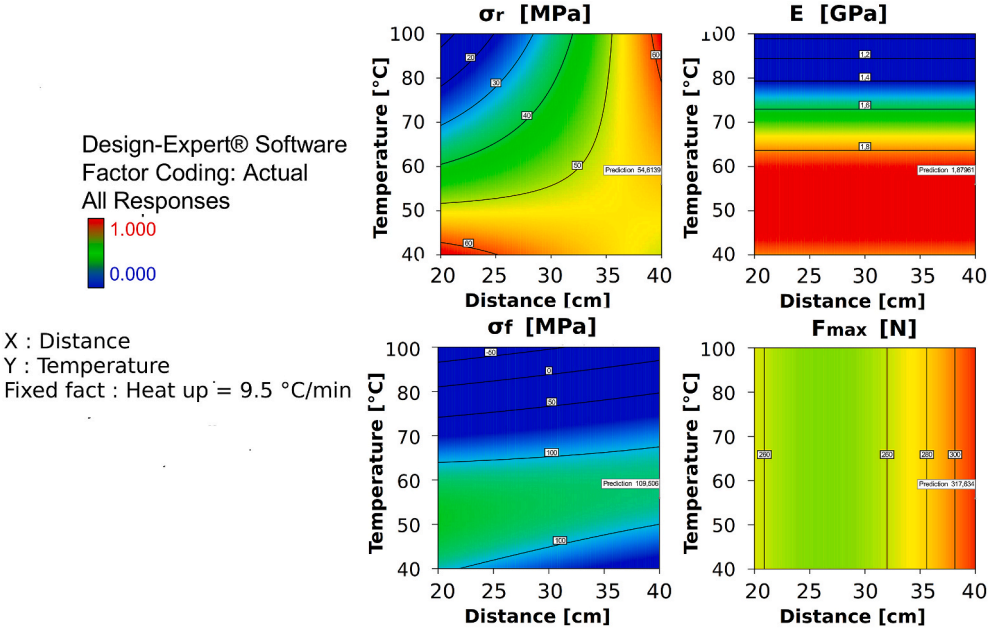

Fig. 14. Influence of temperature and distance on the results from the optimization.

parameters to propose an adhesive with the highest adhesion possible. This can be achieved thanks to the DoE software by weighting the importance of the different answers: the weight of the adherence property is 5, whereas the weight for the other properties is 1. Fig. 13 shows the results (factors and responses) of this optimization.

It should be noted that in this second optimization, the optimal parameters are different from those in the previous one. That is, the distance used is 40 cm with an induced adhesive temperature of around 60°C and a heating rate of 9.5°C/min. These parameters allow obtaining an excellent level of adhesion (very close to the highest possible value) and maintaining an average desirability level of 80%. It is also true that the induced temperature is high compared to the industrial constraints. Fig. 14 shows the influence of temperature and distance parameter evolution on this optimization as a 2D plot.

In this optimization, modifying the lamp parameters leads to a strong variation in the response. Therefore, it is possible to propose parameters that can result in maximized adhesion, but with less consistent mechanical properties.

4. Conclusion

In this study, we focused on the mechanical properties (adherence, tensile strength and modulus, and flexural strength and modulus) of a model adhesive after IR curing. The mechanical properties studied were determined for an IR-cured model adhesive (according to the conditions of the reference test in this study: IR-Φ_{Auto}) compared to pure thermal curing at the same temperature (50°C). The results showed that the adherence properties and tensile and flexural moduli have not been modified by the IR radiation. In contrast, the tensile and flexural strength at break increased when IR curing was used, with an increase of 60% and 20%, respectively, for tensile and three-point bending loads. This difference can be explained by the assumption that IR allows more homogeneous curing and reduces the internal stresses of the model adhesive. In addition, we also studied the most significant factors influencing IR lamp curing. For this purpose, we used a central composite DoE with distance, induced temperature, and heating rate as factors. The results of the DoE are the five mechanical properties studied so far (adherence, tensile strength at break and modulus, and flexural strength at break and modulus). Generally, the DoE allowed us to determine the significant factors for each of the responses by proposing a mathematical model for predicting the values of the mechanical properties. The results further showed that the prediction of the mechanical properties for the IR-Φ_{Auto} reference test is in line with the values obtained experimentally, proving that the suggested model is valid. In addition, determining the significant factors showed that the improvements in the tensile and flexural strength at break after IR curing can be explained by the nonthermal effect of IR radiation. Finally, an optimization of the experimental parameters (i.e., factors) was proposed according to several scenarios: either for a process-oriented optimization (the lowest possible temperature with the highest possible mechanical properties) or for a product-oriented optimization (the highest possible properties). This allowed submitting different parameters for using an IR lamp depending on the properties of the model adhesive required.

Appendix A. Results of adherence, tensile and flexural strength, tensile and flexural modulus

Number	Tensile Strength (MPa)	Tensile modulus (GPa)	Flexural Strength (MPa)	Flexural modulus (GPa)	Adherence (N)
DoE-01	46 ± 3	1.8 ± 0.1	127 ± 16	3.0 ± 0.6	202 ± 7
DoE-02	56 ± 3	1.8 ± 0.1	177 ± 16	4.5 ± 0.6	216 ± 7
DoE-03	44 ± 3	1.8 ± 0.1	160 ± 16	3.6 ± 0.6	222 ± 7
DoE-04	46 ± 3	1.9 ± 0.1	146 ± 16	3.8 ± 0.6	207 ± 7
DoE-05	49 ± 3	1.8 ± 0.1	161 ± 16	3.5 ± 0.6	212 ± 7
DoE-06	45 ± 3	1.8 ± 0.1	130 ± 16	3.5 ± 0.6	201 ± 7
DoE-07	56 ± 3	1.7 ± 0.1	110 ± 16	3.4 ± 0.6	225 ± 7
DoE-08	63 ± 3	1.9 ± 0.1	146 ± 16	3.9 ± 0.6	155 ± 7
DoE-09	53 ± 3	1.6 ± 0.1	138 ± 16	3.5 ± 0.6	151 ± 7
DoE-10	57 ± 3	1.5 ± 0.1	130 ± 16	3.2 ± 0.6	106 ± 7
DoE-11	45 ± 3	1.6 ± 0.1	135 ± 16	3.9 ± 0.6	210 ± 7
DoE-12	49 ± 3	1.5 ± 0.1	144 ± 16	3.8 ± 0.6	207 ± 7
DoE-13	45 ± 3	1.7 ± 0.1	140 ± 16	3.1 ± 0.6	245 ± 7
DoE-14	22 ± 3	1.6 ± 0.1	143 ± 16	4.0 ± 0.6	327 ± 7
DoE-15	34 ± 3	1.4 ± 0.1	114 ± 16	3.3 ± 0.6	149 ± 7
DoE-16	40 ± 3	1.7 ± 0.1	129 ± 16	3.4 ± 0.6	276 ± 7
DoE-17	22 ± 3	1.4 ± 0.1	83 ± 16	2.1 ± 0.6	205 ± 7
DoE-18	31 ± 3	1.6 ± 0.1	91 ± 16	3.0 ± 0.6	209 ± 7
DoE-19	36 ± 3	1.8 ± 0.1	76 ± 16	3.1 ± 0.6	248 ± 7
DoE-20	41 ± 3	1.6 ± 0.1	78 ± 16	2.7 ± 0.6	267 ± 7
DoE-21	34 ± 3	1.6 ± 0.1	105 ± 16	2.9 ± 0.6	286 ± 7
DoE-22	30 ± 3	1.7 ± 0.1	106 ± 16	3.1 ± 0.6	201 ± 7

Appendix B. Infrared lamp emitter spectrum and the measurement of the temperature of the sample when the set point is 50°C

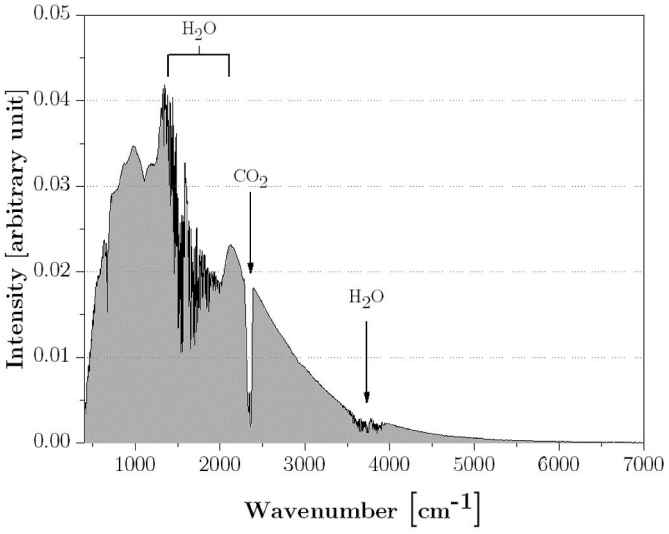

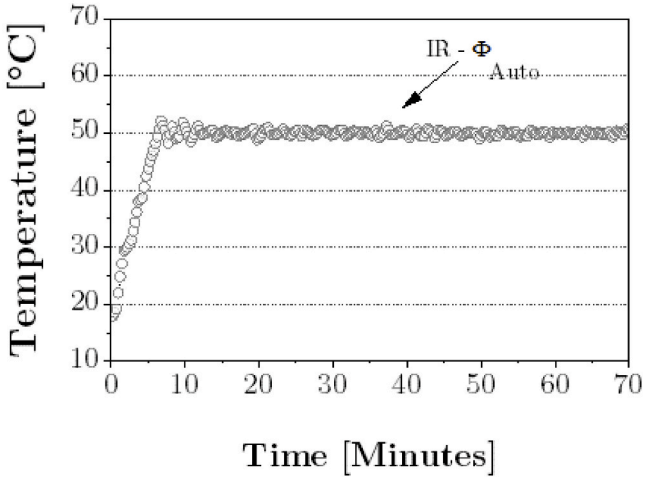

References

[1] Anes V, Pedro R, Henriques E, Freitas M, Reis L. Bonded joints of dissimilar adherends at very low temperatures - an adhesive selection approach. Theor Appl Fract Mech 2016;85:99–112.

[2] Javadi A, Mehr HS, Sobani M, Soucek MD. Cure-on-command technology: a review of the current state of the art. Prog Org Coating 2016;100:2–31.

[3] Yungwirth J, Christian D Wetzel, Eric M, Sands James. Induction curing of a Phase-Toughened adhesive. Army Res. Lab. ARL-TR-299; 2003. p. 30.

[4] Fink BK, McKnight SH. Ferromagnetic nano-particulate and conductive mesh susceptors for induction-based repair of composites. Army Res. Lab. 1998;298:7.

[5] Yarlagadda S, Fink BK, Gillespie JW. Resistive susciptor design for uniform heating during induction bonding of composites. J Compos Mater 1999;33:928–40.

[6] Jacob J, Chia LHL, Boey FYC. Review: thermal and non-thermal interaction of microwave radiation with materials. J Mater Sci 1995;30:5321–7.

[7] Galema SA. Microwave chemistry. Chem Soc Rev 1997;26:233–8.

[8] Marand E, Baker KR, Graybeal JD. Comparison of reaction mechanisms of epoxy resins undergoing thermal and microwave cure from in situ measurements of microwave dielectric properties and infrared spectroscopy. Macromolecules 1992; 25:2243–52.

[9] Yarlagadda Cheok. Study on the microwave curing of adhesive joints using a temperature-controlled feedback system. J Mater Process Technol 1999;91: 128–49.

[10] Majetich G, Hicks R. *Applications of microwave-accelerated organic synthesis*, Radiat. Phys Chem 1995;45:567–79.

[11] Ellis B. Chemistry and Technology of epoxy resins. Dordrecht: Springer Science; 1993.

[12] Petrie EM. Handbook of adhesives and sealants. New York: Mc Gaw-Hill; 2007.

[13] Moreau N. UV-cured hybrid sol-gel coaings for corrosion protection of aeronautical metallic substrates, Thesis from the ". ": Université de Haute-Alsace; 2012.

[14] Belhamra A, Diabi R, Moussaoui A. Technology and applications of infrared heating in the industrial area. J Eng Appl Sci 2007;7:1183–7.

[15] Kiran Kumar P, V Raghavendra N, Sridhara BK. Development of infrared radiation curing system for fiber reinforced polymer composites: an experimental investigation. Indian J Eng Mater Sci 2011;18:24–30.

[16] Genty S, Tingaut P, Aufray M. Fast polymerization at low temperature of an infrared radiation cured epoxy-amine adhesive. Thermochim Acta 2018;666: 27–35.

[17] Bruno Comoglio. Method of sealing a hollow structure, for example a fuel tank for an aircraft. WO 03/076158 A1. 2003.

[18] Roche AA, Behme AK, Solomon JS. A three-point flexure test configuration for improved sensitivity to metal/adhesive interfacial phenomena. Int J Adhesion Adhes 1982;2:249–54.

[19] Roche AA, Dole P, Bouzziri M. Measurement of the practical adhesion of paint coatings to metallic sheets by the pull-off and three-point flexure tests. J Adhes Sci Technol 1994;8:587–609.

[20] Bouchet J, Roche A-A. The formation of epoxy/metal interphases: mechanisms and their role in practical adhesion. J Adhes 2002;78:799–830.

[21] Sauvage J-B, Aufray M, Jeandrau J-P, Chalandon P, Poquillon D, Nardin M. Using the 3-point bending method to study failure initiation in epoxide-aluminum joints. Int J Adhesion Adhes 2017;75:181–9.

[22] Genty S, Sauvage J-B, Tingaut P, Aufray Maelenn. Experimental and statistical study of three adherence tests for an epoxy-amine/aluminum alloy system: pull-Off, Single Lap Joint and Three-Point Bending tests. Int J Adhesion Adhes 2017;79: 50–8.

[23] Kumar PK, Raghavendra NV, Sridhara BK. Optimization of infrared radiation cure process parameters for glass fiber reinforced polymer composites. Mater Des 2011; 32:1129–37.

[24] Aufray M, Roche AA. Properties of the interphase epoxy – amine/metal : influences from the nature of the amine and the metal. Adhes. Curr. Res. Appl. 2006:89–102.

[25] Roche AA, Bouchet J, Bentadjine S. Formation of epoxy-diamine/metal interphases. Int J Adhesion Adhes 2002;22:431–41.
[26] Xu X, Wang X, Wei R, Du S. Effect of microwave curing process on the flexural strength and interlaminar shear strength of carbon fiber/bismaleimide composites. Compos Sci Technol 2016;123:10–6. 030.
[27] Johnston K, Pavuluri SK, Leonard MT, Desmulliez MPY, Arrighi V. Microwave and thermal curing of an epoxy resin for microelectronic applications. Thermochim Acta 2015;616:100–9.